IMPACT OF URBAN EXPANSION ON SURFACE TEMPERATURE IN BAGHDAD, IRAQ USING REMOTE SENSING AND GIS TECHNIQUES

Salah A. H. Saleh
Department of Physics, College of Science, Al-Nahrain University.

Abstract

Baghdad city has experienced a rapid urban expansion over the last decades due to accelerated economic growth. This paper reports an investigation into the application of the integration of remote sensing and geographic information systems (GIS) for detecting urban built up growth for the period 1961-2002, and evaluate its impact on surface temperature in Baghdad city.

The purpose of this study is to analysis and verifies the spatial distribution property of the surface temperature with urban spatial information, related with land cover / land use and NDVI using remotely sensed data and GIS. Surface temperature, land cover pattern and NDVI were extracted from Landsat7 ETM + data. Then surface temperatures, was linked to land use data of Baghdad region for further investigations of the relationship between temperature behavior and urban structures. The Normalized Difference Vegetation Index (NDVI) was used to examine the relation between thermal behavior and vegetation cover amount.

The results showed that the negative average correlation more than 85 % was identified by the results from the correlation and regression analysis of the extracted surface temperature from Landsat data image with NDVI. Also this research verified the distribution of urban surface temperature was very different depends on various land cover type of surrounding areas. Water and forest cover types show low day temperature differences compared to residential, commercial cover types.

The integration of remote sensing and GIS was found to be effective in monitoring and analyzing urban growth patterns and in evaluating urbanization impact on surface temperature.

Introduction

Land covers, as the biophysical state of the earth's surface and immediate subsurface, are sources for most of the material and energy movements and interactions between the geosphere and biosphere. Changes in land cover include changes in biotic diversity, actual and potential primary productivity, soil quality, runoff, and sedimentation rates (Steven et al. 1992), and cannot be well understood without the knowledge of land use change that drives them. Therefore, land use and land cover changes have environmental implications at local and regional levels, and perhaps are linked to the global environmental process. Because of the interrelated nature of the elements of the natural environment, the direct effects on one element may cause indirect effects on others. Urbanization, the conversion of other types of land to uses associated with growth of populations and economy, is a main type of land use and land cover change in human history. It has a great impact on climate. By covering with buildings, roads and other impervious surfaces, urban areas generally have higher solar radiation absorption, and a greater thermal capacity and conductivity, so that heat is stored during the day and released by night. Therefore, urban areas tend to experience a relatively higher temperature compared with the surrounding rural areas. This thermal difference, in conjunction with waste heat released from urban houses, transportation and industry, contribute to the development of urban heat island (UHI). The temperature difference between the urban and the rural areas are usually modest, averaging less than 1 °C, but occasionally rising to several degrees with special urban, topographical and meteorological conditions (Mather, 1986).

The development of social environmental from the agricultural society to the industrial one has caused the changes of topography and weather and landscape of urban areas. These changes of weather are analyzed the correlation of the ground weather observatory with land use data.

In Baghdad, land use and land cover patterns have undergone a fundamental change due to accelerated expansion since 1958. Urban growth has been speeded up, and extreme stress to the environment has occurred. This is particularly true in the city where massive agricultural land is disappearing each year, converting to urban or related uses. Evaluating the magnitude and pattern of all Iraq's urban growth is an urgent need. Furthermore, because of the lack of appropriate land use planning and the measures for sustainable development, random urban growth has been creating severe environmental consequences. Thus, there also is a need to assess the environmental impact of the rapid urban expansion.

The integration of remote sensing and geographic information systems (GIS) has been widely applied and been recognized as a powerful and effective tool in detecting urban land use and land cover change (Ehlers et al., 1990; Treitz et al., 1992; Harris and Ventura, 1995). Satellite remote sensing collects multispectral, multiresolution and multi-temporal data, and turns them into information valuable for understanding and monitoring urban land processes and for building urban land cover datasets. GIS technology provides a flexible environment for entering, analyzing and displaying digital data from various sources necessary for urban feature identification, change detection and database development. However, few of the urban growth studies have linked to post-change detection environmental impact analysis. The question of how to develop an operational procedure using the existing techniques of remote sensing and GIS for examining environmental impacts of rapid urban growth remains to be answered.

The goal of this research is to demonstrate the integrated use of remote sensing and GIS in evaluate urban growth patterns in the Baghdad city and to analyze the impact of the urban growth on surface temperature. The other objectives of this paper is to apply satellite data to analyze the change of surface temperature derived from Landsat 7 ETM+ thermal imagery acquired in 2002. The thermal band of the satellite image was transformed into surface temperature values and these values were intersected with land use cover classes. Multivariate statistical methods were applied to analyze. Also, this research is aim to identify the spatial distribution characteristics of urban surface temperatures environments by analyzing the surface temperature distribution patterns in term of present land cover states and NDVI.

Study Area

Baghdad is the capital and the biggest city of Iraq. Baghdad history starts during the Islamic era. The city was founded first on the west side of Tigris River in the year 762 A.D by caliph Al-Mansour, it was known as the round city. The new developments in Baghdad began in 1915 when Rashid Street was built through Rusafa side, which became the center of Baghdad at that time. Shortly after that new business streets (like Al-Kifah, Al-Sheik Omar in 1936 and Al-Khulafa in 1954) were constructed in the center of Baghdad. These streets shaped the city center pattern which we know now.

After 1927 many residential quarters founded for both side of Baghdad, new low income communities founded since 1957 for new migrants from central and southern part of Iraq. The constructions of dams as a flood protection gave unlimited aerial expansion for city population and changed the boundary of the city. The size of city was not large enough to cope with the increased population and their activities. Forty years later the city expanded to the Rusafa side. The extension was generally towards the north and to the south. The greater factor that limited the shape of the city growth was the dangerous flood of Tigris River, and several dikes have been built to protect the city.

Baghdad city population growth was reported through successive census during last 60 years; it was notice that the percentage of Baghdad population to that of total Iraq population was increasing continuously (from 10% in 1947 to more than 25% now). The population density of Baghdad city react to 5233 prs/km^2 and it is between 6-190 prs/km^2 for other Iraqi cities.

Table (1)
Population growth for Baghdad.

Census year	Baghdad population	% to Iraq population
1947	503000	10.5
1957	1000000	16.6
1967	1884151	22.0
1977	2823844	23.5
1987	3844608	24.1
1997	5104421	24.9

Baghdad is located in the central parts of Iraq on the both sides of Tigris River. Diala River forms the eastern boundary of the city. Within the city there are manned canals and pounds. Baghdad is suited in a plain area of an elevation between 31-39 m above sea level. So, no natural boundaries exists that limits the aerial extension of the city.

The climate of Baghdad region (which is part of the a plain area at the central of Iraq and has same climatic characteristics) may be defined as a semi arid, subtropical and continental, dry, hot and long summer cool winters and short springs. The maximum recorded temperature was 51 ^{o}C in summer while the minimum was (–10 ^{o}C). The average maximum temperature for the last 30 year is 31.95 ^{o}C and average minimum temperature is 18.05 ^{o}C for the same period.

The sun is the main temperature source. It affects the climatic of city according to the time length of exposure and seasonal variations. The daily average of sunshine duration is 9.6 hours and daily in coming radiation is 4708 mw cm^{-2}. The total average annual sunny hour during one complete year is about 3500 hours.

Fig.(1) : Map of Baghdad city (2003).

Urban Expansion of Baghdad City

Baghdad city have suffered a rapid urban and radium expansion over the last 60 years due to accelerated economic growth and other factors. Urbanization has great impact on climate and the environmental of the region.

Urban expansion detection of Baghdad city for the period 1961-2002 was conducted using high resolution IKONOS satellite image (1 m resolution) acquired in 2002 (Fig. (2)), and thematic map (Bus Map) dated 1961 (Fig.(3)). Fig.(4) shows the process followed in this part of the work.

Fig.(2) : IKONOS image (2002).

Fig.(3) : Baghdad map (1961).

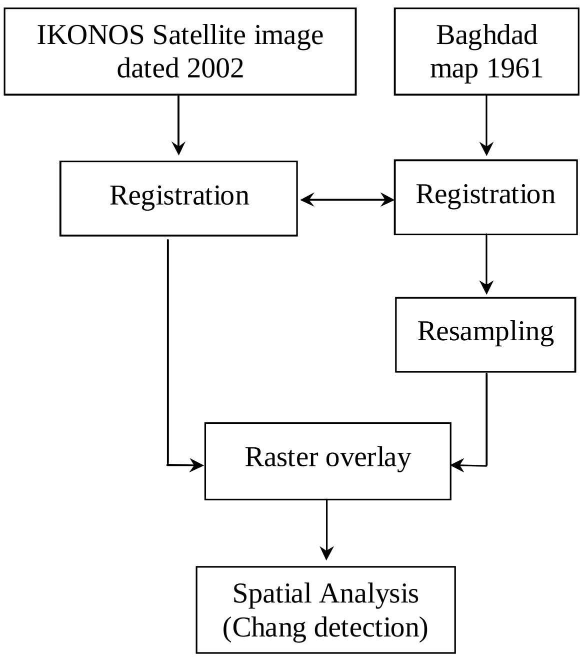

Fig.(4) : Block diagram of urban expansion detection steps.

Satellite image (2002) and Baghdad map (1961) had to be registered to each other firstly. Satellite image was already geometrically corrected and registered using following parameter: Datum = WGS84, Spheroid = WGS84, projection = UTM and Zone = 38. The output geometric corrected image (photomap) is used later for spatial analysis.

Twelve Ground Control Points (GPCPs) distributed through out the satellite image had selected. Then linear transformation was applied to transform map coordinates the geo-referenced image coordinates. The root mean square error (RMS_{error}) was equal to 0.25 pixels. Then, resampling operation for registered map was conducted by nearest neighbor method. ERDAS 8.4 well known image processing software is used for the operation of registration process.

Raster overlay process (spatial analysis) as is applied as urban expansion detection method for Baghdad city at the period 1961-2002 by using ARC VIEW 3.3. Fig. (5) shows the out of overlying 1961 map to 2002 satellite image.

Fig.(5) : Overlying of 1961 map over 2002 satellite image.

From this figure we noticed that there was randomly growth (expansion) in all direction of the city. The major expansion was in south and west of the city. Diala River in the south east of Baghdad limited the expansion in that direction, it works as natural boundary for the city.

For calculation of Baghdad areas in 1961 and 2002, visual screen digitization technique was used. The urban built up areas were identified as polygons as it shown in Figs.(6,7).

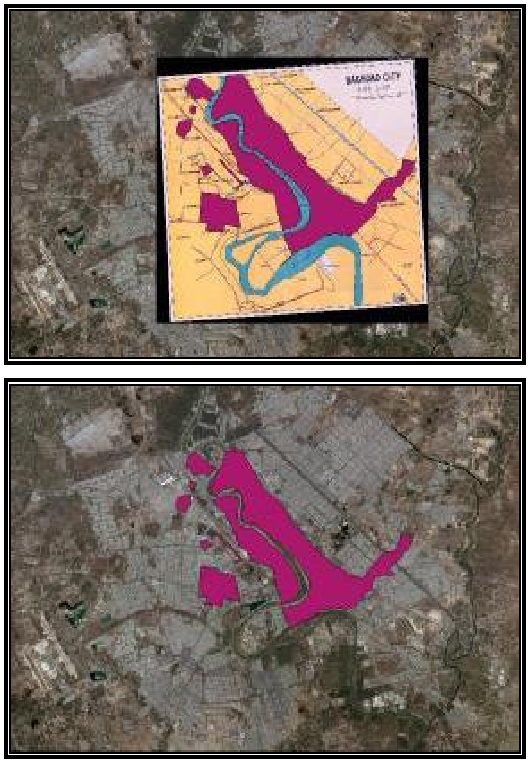

Fig.(6) : Location of Baghdad urban area (1961).

Fig.(7) : Location of Baghdad urban area (2002).

Then the areas of urban polygons for 1961 and 2002 were calculated. It was found that the area of Baghdad in 1961 was 53.16 km^2, and equal to 278.542 km^2. That means the built up urban area of Baghdad increased randomly more than five times in the period 1961-2002, the yearly increasing rate was about 0.131.

Impact of Urban Expansion on Surface Temperature

Lansat7 ETM+ image and digital maps were used in order to effectively identify the spatial distribution characteristics of land cover/land use classes and surface temperature for the city of Baghdad. Landsat 7 ETM+ scenes dated 6/9/2002 of Baghdad was analyzed with respect to surface temperature. The work of this research carried out as following process in Fig.(8):

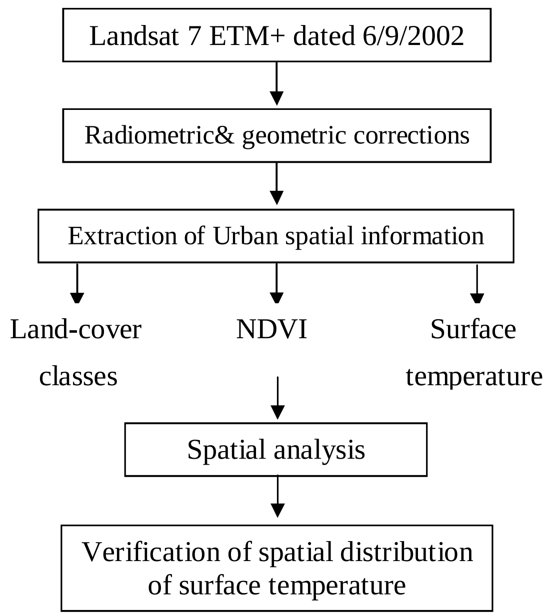

Fig.(8) : Flowchart showing the major steps of research.

Table (2)
Spectral and spatial resolution of the actual Landsat7 ETM+ sensors.

Bands	Spectral resolution	spatial resolution
Band1	0.450-0.515 µm	30 m
Band2	0.525-0.605 µm	30m
Band3	0.630-0.690 µm	30m
Band4	0.775-0.900 µm	30m
Band5	1.550-1.750 µm	30m
Band6-1	10.40-12.50 µm	60m
Band6-2	10.40-12.50 µm	60m
Band7	2.090-2.350 µm	30m
Band8	0.520-0.900 µm	15m

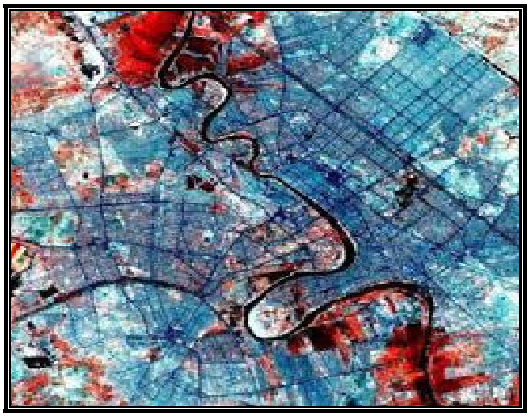

Fig.(9) : False Color Composite of Baghdad City (study Area).

Histogram adjustment have used for minimizing atmospheric effect. This simple method is based primarily on the fact that infrared data are largely free of atmospheric scattering effects, whereas the visible regions are strongly influenced by them. Normally the data collected in visible wavelengths have higher minimum value due to the increased atmosphere scattering taking place in these wavelengths. So if the histogram is shifted to the left so that the effect of atmospheric scattering will be somewhat minimized. This simple algorithm models the first order effect of atmospheric scattering or haze.

1. Land cover classification for urban expansion:

By using ENVI software, the image was radiometrically corrected and enhanced using relative correction and enhancement method (histogram adjustment), to increase the volume of visible information. Unsupervised classification by K-mean method was firstly used to have an idea about spectral pattern of the area.

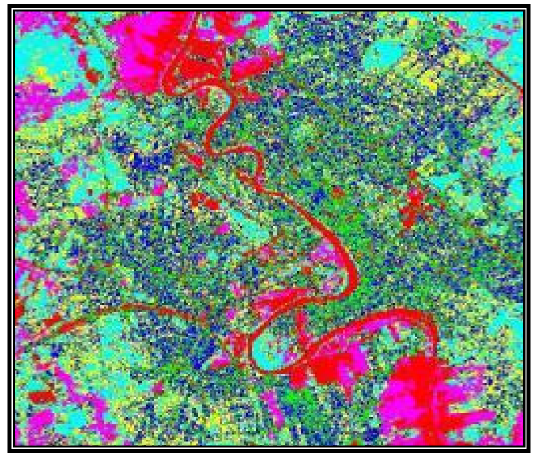

Fig.(10) : Unsupervised classification by K-mean method.

Land use/cover pattern were mapped by supervised classification of landsat7 ETM+ data. After selecting training areas, a supervised classification with the maximum likelihood algorithm was conducted to classify the Landsat images using bands 2 (green), 3 (red) and 4 (near-infrared). The study area was classified to eight land use and land cover classes.

The accuracy of the classification was verified by field checking or comparing with existing land use and cover maps that have been field-checked. Then the results were used as basic data for the analysis of the surface temperature by land cover/use pattern.

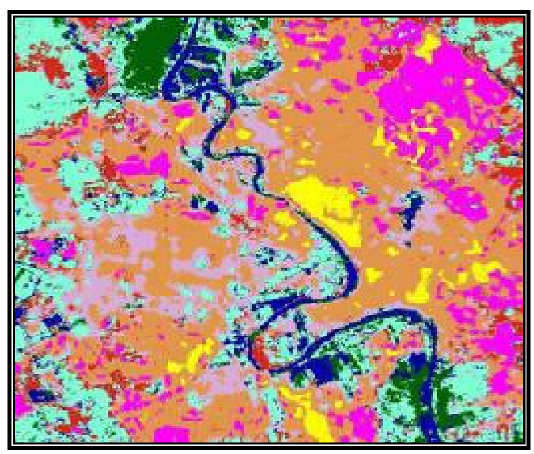

Fig.(11) : Supervised classification image by the maximum likelihood algorithm.

Table (3)
Supervised classification statistics summary report for images.

Class name	*Class color*	*Number of pixels*	*Percentage %*
Orchard		7974	5.64
Water		8958	6.14
Residential-high		15712	10.77
Commercial		5191	3.55
Barren land		9977	6.84
Residential- med		49688	34.06
Residential- low		19549	13.40
Open Area		28811	19.75

Clearly, the used landsat data have reasonably high accuracy, and thus are sufficient for urban growth detection. Table (3) shows the land use and land cover classification results. From this table, it is clear that there has been a considerable increasing in built up area than other classes.

Residential, commercial and industrial areas occupied major of study area which about 62% of total area, while only 38% of total area for other land cover pattern (water, orchards, barren land and open areas).

Urban development usually gives rise to a dramatic change of the Earth's surface, as natural vegetation is removed and replaced by non-evaporating and non-transpiring surfaces such as metal, asphalt and concrete. This alteration will inevitably result in the redistribution of incoming solar radiation, and induce the urban–rural contrast in surface radiance and air temperature. The difference in ambient air temperature between an urban and its surrounding rural area is known as the effect of UHI. Given the relationship between surface radiant temperature and the texture of land cover, the impact of urban development on surface temperature can be assessed. Studies on surface temperature characteristics of urban areas using satellite remote sensing data have been conducted primarily using NOAA AVHRR data (Balling and Brazell 1988, Roth et al. 1989, Gallo et al. 1993a). The spatial resolution of NOAA (1.1KM) data is found suitable only for small-scale urban temperature mapping. The much higher resolution (120 m) Landsat TM thermal infrared data were seldom used to derive surface temperature. Recently, Carnahan and Larson (1990) have used the TM thermal infrared data to observe the temperature differences between urban and rural areas.

2. Thermal signatures of land cover types:

In order to understand the impacts of land use/cover change on surface radiant temperature, the characteristics of the thermal signatures of each land cover type must be studied first. For the surface temperature estimation, the radiation emitted from the target on the surface is measured by using thermal infrared region (10.4-12.5 μm) of landsat 7 ETM+ image. Surface temperature of wide areas can be extracted under assumption that satellite sensor should have proximity to the black body. In this study we estimated the surface temperature using NASA model.

The digital numbers were transformed into absolute radiance (see: Schott & Volchock, 1985), Using:

$$L(\lambda) = GAIN \times DN + OFFSET \quad \ldots\ldots\ldots\ldots(1)$$

Which can also be expressed as:

$$L\lambda = (Lmax - Lmin)/255 \times DN + Lmin \ldots(2)$$

Where: Lλ is the spectral radiance, Lmin and Lmax [mW $cm^{-2}sr^{-1}\mu m^{-1}$] are spectral radiances for each band at digital numbers 0 and 255 respectively. For the new sensors in TM 7 the following reference values are given:

ETM+ Spectral Radiance Range:

Low Gain: Lmin – 0.0 Lmax – 17.04 watts/ (meter squared×ster×μm)

High Gain: Lmin – 3.2 Lmax – 12.65 watts/ (meter squared×ster×μm)

The spectral radiances (Lλ) were converted into effective at-satellite temperatures T by

$$T = K2 / \ln (K1 / L\lambda + 1) \ldots\ldots\ldots\ldots\ldots\ldots(3)$$

Where: K2 = 1260,56 K were taken; for Landsat ETM+ the NASA – handbook gives K1 = 666,09 $w \times m^{-2} \times sr^{-1} \times \mu m^{-1}$ and K2=1282.71 K respectively. For Landsat

ETM+ the values were also given in the header information of the thermal bands.

Then, corrections for emissivity (ε) were applied to the radiant temperatures according to the nature of land cover. In general, vegetated areas were given a value of 0.95 and non-vegetated areas 0.92 (Nichol 1994). The emissivity corrected surface temperature can be computed as follows (Artis and Carnahan 1982):

$$Ts = T(K)/ (1 + (\lambda T(K)/\alpha) \ln \varepsilon \ldots\ldots\ldots\ldots(4)$$

Where λ = wavelength of emitted radiance (for which the peak response and the average of the limiting wavelengths (λ=11.5 μm) (Markham and Barker 1985) will be used, α = hc/K (1.438×10^{-2} m K), K = Stefan Boltzmann's constant (1.38×10^{-23}J K^{-1}), h = Planck's constant (6.26×10^{-34}J s), and c = velocity of light (2.998×10^{8} m s^{-1}).

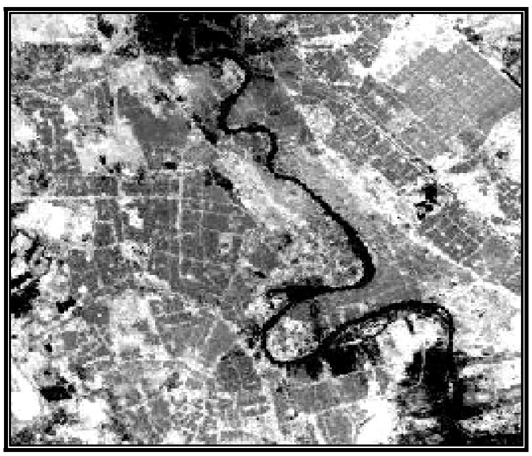

Fig.(12): Thermal image (band 6) for study area.

Table (4)
The average surface temperature per land-cover class.

Class Name	Mean DN Value	STD	Temperature °C
Orchard	5.02	10.05	33.75
Water	1.83	3.412	31.50
Residential-high	165.33	21.82	52.11
Commercial	171.03	19.63	52.31
Paved & Barren land	104.70	10.61	46.97
Residential-med	119.37	18.37	49.01
Residential-low	94.50	26.47	43.25
Open Area	127.01	51.47	45.31

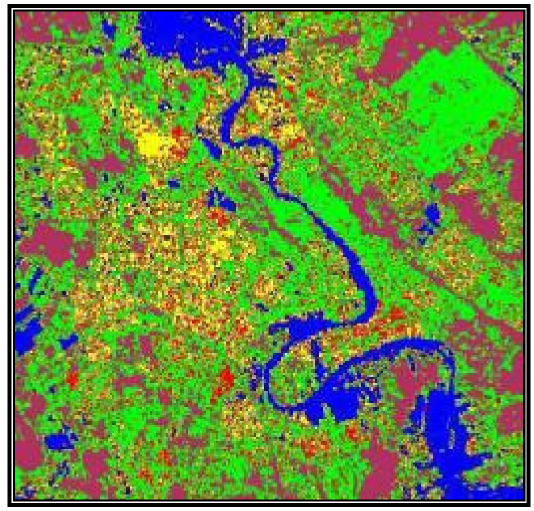

Fig.(13) : Classification of thermal image by level slicing technique.

Table (5)
Level slice classification statistics summary report for thermal image.

Class Name	Color	Temperature
Water & Orchard	(blue)	30-35 °C
Commercial & Residential- high	(green)	52-55 °C
Paved & Barren land	(purple)	45-46 °C
Residential- med	(red)	49-50 °C
Residential- low	(yellow)	47-48 °C

Commercial area had the highest surface temperature, while water bodies have the lowest surface temperature. The range of 30-35 ^{0} c is widely distributed over the orchard lands and water bodies. Meanwhile the major commercial, industrial district (along the two sides of Tigris River and in the center of Baghdad) and the residential area of high density had the level of high temperature with range 50-55 °C. These areas obviously present the different distributions of surface temperature from those of lower temperature of other urban area. Also these results will be explained with correlation analysis among land cover classes and NDVI factors.

According to the results shown in figures (6,7), the average values of radiant surface temperatures by land cover type are summarized in Tables (4,5). Commercial area had the highest surface temperature, while water bodies have the lowest surface temperature. The range of 30-35 ^{o}C is widely distributed over the orchard lands and water bodies. Meanwhile the major commercial and high density residential area had the level of high temperature with range 50 - 55 ^{o}C. These areas obviously present the different distributions of surface temperature from those of lower temperature of other urban area.

It is clear that, urban or built-up land exhibits the highest surface radiant temperature followed by barren land. This implies that urban development does bring up surface radiant temperature by replacing natural vegetation with non-evaporating, non-transpiring surfaces such as stone, metal and concrete**.** The lowest radiant temperature is found in water bodies, followed by orchards. This different pattern is primarily attributed to the differences in solar illumination, the state of vegetation, and atmospheric influences on the remotely sensed TM data set. The difference in data acquisition season is clearly reflected in the surface radiant temperatures of water bodies. The radiant temperature of water bodies is higher than that of orchards in winter, while in summer lower than that of forest.

Orchards show a considerably low radiant temperature because dense vegetation can reduce amount of heat stored in the soil and surface structures through transpiration. The influence of surface soil water content and vegetation contribute to a broad variation in their surface radiant temperature value. Given the relationship between surface radiant temperature and the texture of land cover that is influenced by land use, changes in land use and land cover can have a profound effect on the surface radiant temperature in a region.

3. Normalized Difference Vegetation Index (NDVI):

Because normalized difference vegetation index (NDVI) has been found to be a good indicator of surface radiant temperature (Nemani and Running 1989, Gallo et al. 1993b, Gillies and Carlson 1995, Lo et al. 1997), a NDVI image was computed from visible (0.63–0.69 μm) and near-infrared (0.77–0.90 μm) data of the Landsat TM, using the following formula:

$$NDVI = TM\,4 - TM\,3 / TM\,4 + TM\,3 \quad \ldots(5)$$

The original NDVI had the values between −1 to +1, but we transformed NDVI values into image of 8 bit (0-255) value. The resultant NDVI image was correlated with the land use/cover change and surface temperature map extracted from landsat image to study how all these changes have interacted.

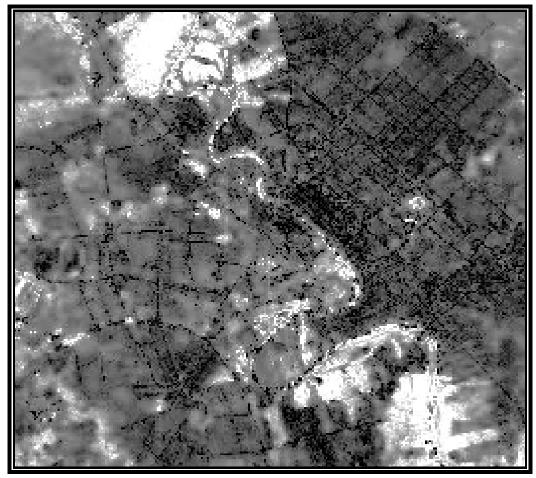

Fig. (15) : NDVI image for Baghdad city (study area).

The average NDVI value for each land cover patterns then is found and given in Table (6).

Table (6)
The average NDVI per land cover/ land use classes.

Class Name	Mean NDVI Value	STD
Orchard	248.46	18.15
Water	183.92	78.93
Residential-high	74.40	13.04
Commercial	31.95	29.20
Paved & Barren land	57.83	12.04
Residential-med	75.158	30.75
Residential-low	108.96	16.03
Open Area	159.638	24.06

As shown in the above table orchard area had the highest NDVI value while commercial area had the lowest NDVI because this area is located in the in the center of Baghdad, therefore, there were just a few green spaces. Residential and paved areas also have low value of NDVI due to Urban development which usually gives rise to a dramatic change of the Earth's surface, as natural vegetation is removed and replaced by non-evaporating and non-transpiring surfaces such as metal, asphalt and concrete.

4. Correlation analysis between Surface Temperature and NDVI:

It is well known that the NDVI is negative correlated with surface radiant temperature (Lo et al., 1997). The relationship between surface radiance temperature and NDVI was investigated for each land cover type through correlation analysis. Table (7) shows the analysis between surface temperature and NDVI with respect to land cover/use type. It is apparent from the table that surface temperature values tend to negatively correlate with NDVI values for all land cover types.

Table (7)
Surface temperature, NDVI per land use \ cover classes.

Class Name	Number of pixels (area)	Average NDVI	Temperature (°C)
Orchard	7974	248.46	33.75
Water	8958	183.92	31.50
Residential-high	15712	74.40	52.11
Commercial	5191	31.95	52.31
Paved & Barren land	9977	57.83	46.97
Residential-med	49688	75.158	49.01
Residential-low	19549	108.96	43.25
Open Area	28811	159.638	45.31

These correlations can be visualized by plotting the corresponding mean surface temperature values for all land cover types with NDVI into scattergrams plot.

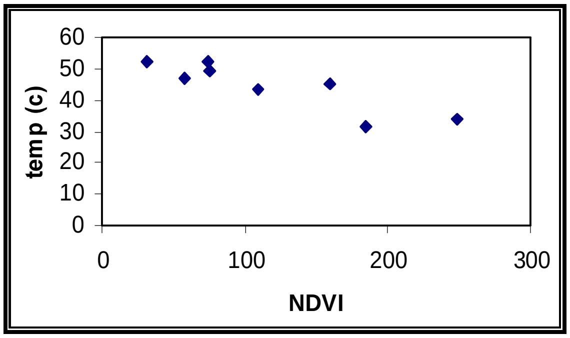

Fig.(16) : Scattergram of average surface temperature vs. NDVI (r = –0.879).

From Fig. (16) water and orchard cover types are located in the right lower corner of the diagram, low residential density and service areas are located in the centre of the diagram (medium values for both parameters, NDVI surface temperature), while the commercial and residential (high and medium density) areas are located at the upper left corner of the diagram. In other words: the NDVI confirms the cluster structure of land cover types derived from surface temperatures

However the correlation analysis cannot explain the correlation among variables and their correlative degree. For these explanations linear regression analysis was carried out to bring out the regression equation.

Regression equation	R	R^2
Y = –0.0939 X + 55.308	–0.879	0.7741

The strong negative correlation (-0.879) between surface radiance temperature and NDVI implies that the higher biomass a land cover has, the lower the surface temperature. Because of this relationship between surface radiance temperature and NDVI, changes in land use/cover have an indirect impact on surface temperatures through NDVI.

Conclusions

An integrated approach of remote sensing and GIS was applied for evaluation of rapid urban expansion of Baghdad city for the period (19661-2002) and its impact on surface temperature in Baghdad city, Iraq. This study analyzed the spatial distribution of urban surface temperature according to land-cover types and NDVI with remotely sensed data. The results are summarized as:

1- A rapid urban expansion of Baghdad city noticed by remote sensing and GIS over the last decades due to accelerated economic growth. The area of Baghdad was 53.16 km^2 and 278.52 km^2 for the years 1961 and 2002 respectively. The expansion rate was about 0.131 per year.
2- There was randomly growth (expansion) in all direction of Baghdad city for the period 1961-2002. The major expansion was in south and west of the city. Diala River in the south east of Baghdad limited the expansion in that direction.
3- According to results of analyzing the surface temperature in terms of land-cover classification patterns, the commercial and the dense residential area were verified to form the high surface temperature distributions with lowest vegetation cover ratio. The negative correlation more than 85% was identified by the results from correlation analysis of the extracted surface temperature from landsat image with NDVI.
4- The results showed that urban land development raised surface temperature. The spatial pattern of surface temperature distribution was correlated with the pattern of urban expansion. The direct effect of urban land use/cover change on one environmental element can cause indirect effect on the other. The increase of surface radiant temperature was related to the decrease of biomass.
5- The methodology employed in this study provides an alternative to the traditional empirical observation and analysis using in situ data for environmental studies. This methodology should be possible to apply to other regions that undergo a rapid urbanization.
6- The computed surface radiant temperatures by this method may be higher than as they were, since the effects of surface roughness on surface temperature have not been taken into account. Effective measurement of surface temperatures requests to analyze the significance of the nature of surface and its roughness on emissivities.
7- The statistical analysis of thermal information and vegetation indices confirms that each of them contains independent information which should be used for the analysis of urban environment. The change of surface temperature during the year is dependent on surface cover and NDVI which is shown in this work. The emissivity of different land use cover is therefore dependent on NDVI, and because of this, of the vegetation.
8- The integration of remote sensing and GIS was found to be effective in monitoring and analyzing urban growth patterns and in evaluating urbanization impact on surface temperature. The digital image classification coupled with GIS has demonstrated its ability to provide comprehensive information on the nature, rate and location of urban land expansion. Biophysical measurements including surface radiant temperature and biomass can be extracted from Landsat TM images.

References

[1] Artis, D. A., and Carnahan, W. H., 1982, Survey of emissivity variability in thermography of urban areas. Remote Sensing of Environment, 12, 313-329.

[2] Balling, R. C., and Brazell, S. W., 1988, High resolution surface temperature patterns in a Complex urban terrain. Photogrammetric Engineering and Remote Sensing, 54, 1289-1293.

[3] Carnahan, W. H., and Larson, R. C., 1990, An analysis of an urban heat sink. Remote Sensing of Environment, 33, 65-71.

[4] Ehlers, M., Jadkowski, M. A., Howard, R. R., and Brostuen, D. E., 1990, Application of A remote sensing–GIS evaluation of urban expansion SPOT data for regional growth analysis and local planning. Photogrammetric Engineering and Remote Sensing, 56, 175-180.

[5] Gallo, K. P., McNab, A. L., Karl, T. R., Brown, J. F., Hood, J. J., and Tarpley, J. D.,1993a, The use of NOAA AVHRR data for assessment of the urban heat island effect. Journal of Applied Meteorology, 32, 899-908.

[6] Gallo, K. P., McNab, A. L., Karl, T. R., Brown, J. F., Hood, J. J., and Tarpley, J. D.,1993b, The use of a vegetation index for assessment of the urban heat island effect,International Journal of Remote Sensing, 14, 2223-2230.

[7] Gillies, R. R., and Carlson, T. N., 1995, Thermal remote sensing of surface soil water content with partial vegetation cover for incorporation into climate models. Journal of Applied Meteorology, 34, 745-756.

[8] Harris, P. M., and Ventura, S. J., 1995, The integration of geographic data with remotely Sensed imagery to improve classification in an urban area. Photogrammetric Engineering and Remote Sensing, 61, 993-998.

[9] Lo, C. P., Quattrochi, D. A., and Luvall, J. C., 1997, Application of high-resolution thermal infrared remote sensing and GIS to assess the urban heat island effect. International Journal of Remote Sensing, 18, 287-304.

[10] MARKHAM, B. & BARKER, J. L. (1986): Landsat MSS and TM post calibration dynamic ranges, exoatmo-spheric reflectances and at-satellite temperatures. - EOSAT Landsat tech. Notes, 1, p. 3-7, Lanham (EOSAT).

[11] Mather, A. S., 1986, Land Use (London: Longman).

[12] Nemani, R. R., and Running, S. W., 1989, Estimation of regional surface resistance to evapotranspiration from NDVI and thermal-IR AVHRR data. Journal of AppliedMeteorology, 28, 276–284.

[13] Roth, M., Oke, T. R., and Emery, W. J., 1989, Satellite derived urban heat islands from three coastal cities and the utilization of such data in urban climatology. International Journal of Remote Sensing, 10, 1699–1720.

[14] SCHOTT, J.R. & VOLCHOCK, W.J. (1985): Thematic Mapper infrared calibration. Photogramm. Eng. Remote Sensing, 51, 9, p. 1351-1357, Falls Church, VA.

[15] Steffen, W. L., Walker, B. H., Ingram, J. S., and Koch, G. W., 1992, Global change and terrestrial ecosystems: the operational plan. IGBP Report No. 21, International Geosphere-Biosphere Programme, Stockholm.

[16] Treitz, P. M., Howard, P. J., and Gong, P., 1992, Application of satellite and GIS technologies for land-cover and land-use mapping at the rural-urban fringe: a case study. Photogrammetric Engineering and Remote Sensing, 58, 439–448.

[17] Weng, Q., 1998, Local impacts of the post-Mao development strategy: the case of the Zhujiang Delta, southern China. International Journal of Urban and Regional Studies, 22, 425–442.

[18] Yeh, A. G. O., and Li, X., 1996, Urban growth management in the Pear River delta-an integrated remote sensing and GIS approach. ITC Journal, 1, 77–85.

الخلاصة

شهدت مدينة بغداد خلال العقود الأخيرة توسع حضري سريع بسبب النمو الاقتصادي المتسارع مما أثر سلبياً على بيئة المنطقة من خلال الزحف على المناطق الزراعية والبساتين المحيطة بالمدينة. ويهدف هذا البحث الى تقيم تاثير توسع مدينة بغداد على درجات الحرارة السطحية لاصناف الغطاء الارضي باستخدام معلومات الاستشعار عن بعد ونظم المعلومات الجغرافية. حيث تم ومن الصور الفضائية نوع لاندسات 7 استخلاص وتحليل درجات الحرارة وتوزيعها لاصناف الغطاء الارضي لمنطقة الدراسة. ولغرض دراسة تأثير التوسع الحضري على بيئة منطقة مدينة بغداد تم حساب معامل دليل الخضرة النباتية (NDVI) ودرجات الحرارة السطحية لكل صنف من اصناف الغطاء الارضي.

النتائج اظهرت ان هناك توسع عشوائي في المدينة وتحولت مناطق واسعة من البساتين والمزارع الى مناطق حضرية مما ادى الى ظهور علاقة عكسية بين درجات الحرارة السطحية مع (NDVI).